Molecular Neurobiology (2019) 56:8513–8523
https://doi.org/10.1007/s12035-019-01652-3

Coincident Pre- and Post-Synaptic Cortical Remodelling Disengages Episodic Memory from Its Original Context

Gisella Vetere[1,2] · Antonella Borreca[1,3,4] · Annabella Pignataro[1,3] · Giulia Conforto[1] · Michela Giustizieri[5] · Silvia Marinelli[5] · Martine Ammassari-Teule[1,3]

Received: 23 January 2019 / Accepted: 15 May 2019 / Published online: 2 July 2019

Abstract

The view that the neocortex is remotely recruited for long-term episodic memory recall is challenged by data showing that an intense transcriptional and synaptic activity is detected in this region immediately after training. By measuring markers of synaptic activity at recent and remote time points from contextual fear conditioning (CFC), we could show that pre-synaptic changes are selectively detected 1 day post-training when the memory is anchored to the training context. Differently, pre- and post-synaptic changes are detected 14 days post-training when the memory generalizes to other contexts. Confirming that coincident pre- and post-synaptic remodelling mediates the disengagement of memory from its original context, DREADDs-mediated enhancement of cortical neuron activity during CFC training anticipates expression of a schematic memory and observation of bilateral synaptic remodelling. Together, our data show that the plastic properties of cortical synapses vary over time and specialise in relation to the quality of memory.

Keywords Systems consolidation · Episodic memory · Neocortex · Synaptic proteins · Miniature EPSC · Dendritic spines · DREADDs

Introduction

Episodic memory relies on the formation of flexible relational representations that link the single components of a specific experience [1, 2]. Neural traces of these representations are formed and stored in the brain through synaptic rearrangements that have been shown to gradually spread from the hippocampus to the medial regions of the prefrontal cortex [3–5].

This view is, however, challenged by data showing that already 1 h following contextual fear conditioning (CFC), the neocortex undergoes an intense transcriptional activity

Gisella Vetere, Antonella Borreca and Annabella Pignataro contributed equally to this work.

✉ Martine Ammassari-Teule
martine.teule@cnr.it

Gisella Vetere
gisella.vetere@espci.fr

Antonella Borreca
antonella.borreca@gmail.com

Annabella Pignataro
annabellapignataro@gmail.com

Giulia Conforto
cofortogiulia@virgilio.it

Michela Giustizieri
m.giustizieri@ebri.it

Silvia Marinelli
s.marinelli@ebri.it

[1] Department of Experimental Neuroscience, Laboratory of Psychobiology, Fondazione Santa Lucia, via del Fosso di Fiorano 64, 00143 Rome, Italy

[2] Laboratoire Plasticité du Cerveau, ESPCI-Ecole Supérieure de Physique et Chimie Industrielle, Paris, France

[3] Consiglio Nazionale delle Ricerche, Istituto di Biologia Cellulare e Neurobiologia, Rome, Italy

[4] Present address: Consiglio Nazionale delle Ricerche, Istituto di Neuroscienze, Milan, Italy

[5] European Brain Research Institute, Rome, Italy

accompanied by structural and functional neuronal alterations [6]. At the structural level, an enhancement in the length of the active zone of the post-synaptic density, the number of docked synaptic vesicles, and the proportion of mushroom-shaped dendritic spines, is detected although the total number of spines remains unchanged. At the functional level, increased expression of pre-synaptic proteins accompanied by a selective augmentation in the frequency, but not in the amplitude of miniature excitatory post-synaptic currents (mEPSCs), indicates that cortical alterations which develop shortly post-training are prevalently pre-synaptic.

Despite evidence showing that the content of an episodic memory undergoes lifelong modifications which gradually transform the detailed representation of the original episode into a schematic representation [7–9], whether the plastic properties of cortical synapses vary over time and specialise in relation to quality of memory has not been yet examined [10]. Here, we show that cortical synapses are selectively remodelled on their pre-synaptic side 1 day post-training (recent recall) when memory is anchored to the training context. Differently, coincident pre- and post-synaptic remodelling is detected 14 days post-training (remote recall) when the memory generalizes to another context. Confirming that bilateral remodelling of cortical synapses is sufficient to disengage episodic memory from its original context, DREADDs activation of cortical neurons during CFC training allows schematic memory and increased expression of post-synaptic proteins to be observed at recent recall.

Methods

Animals We used male C57BL/6J@Ico (C57) mice and Thy1-GFP-M mice bred on a C57BL/6 background. Mice were 9 weeks old at the beginning of the experiments. They were housed 5 per cage and maintained in a temperature-controlled facility (22 ± 1 °C) on a 12:12 h light-dark cycle with free access to food and water. All experimental procedures were conducted in accordance with the official European Guidelines for the care and use of laboratory animals (86/609/EEC). C57 mice were used for post-training measurements of synaptic protein expression and of their co-localisation. Thy1-GFP-M mice were used for post-training measurements of miniature excitatory post-synaptic currents (mEPSCs) and spine density, and for assessment of behavioural and neural changes after chemogenetic modulation of aCC neuron firing.

Contextual Fear Conditioning Mice were first handled for 3 days in the conditioning room. Contextual fear conditioning (CFC) consisted of one single session of 7 min and began on the next day. Each mouse was placed in a squared conditioning chamber made of a transparent plexiglas cage (28 × 28 × 10 cm) with a removable grid floor made of stainless steel rods. After 120 s of free exploration, each mouse ($N = 78$, 13 per time point) was exposed to a series of 5 non-signalled foot shocks (duration 2 s; intensity 0.7 mA, 60-s apart) delivered through the grid-floor. Pseudo-trained mice ($N = 54$, 9 per time point) were treated identically except that they were not shocked. Fear memory recall tests were run either 1 day or 14 days after the conditioning by returning mice to the conditioning chamber where they were left for 4 min without any foot shock was delivered. To control for the context dependence of memory, four groups of mice ($N = 32$, 8 per group) were used following training. These mice were tested for recent or remote memory in the training context (context A) or in a novel context (context B). They were placed 4 min in context A or context B consisting in a safe cage made of black plastic material with a solid floor. To examine whether early cortical activation by DREADDs could anticipate formation of context-independent memory and post-synaptic remodelling, 7 additional groups of mice ($N = 56$, 8 per group) were trained ($N = 40$, 8 per group) or pseudo-trained ($N = 16$, 8 per group) in context A and directly tested 1 day later in context B. To control that early cortical activation by DREADDs did not affect context-dependent memory, two additional groups of mice ($N = 16$, 8 per group) were trained and tested 1 day later in context A. Behaviour during conditioning and testing was recorded by means of a video camera mounted 60 cm above the ceiling of the cage and connected to a computer equipped with the Ethovision software (Noldus, Wageningen, The Netherlands). The time spent freezing (absence of all but respiratory movements) during each 4-min recall test was used to score fear memory.

Western Blot Trained and pseudo-trained mice were sacrificed by cervical dislocation 1 h after the memory tests run in context A either 1 day or 14 days post-training. Their brains were removed immediately, cut in 1-mm-thick sections using a frozen brain matrix (ASI Instruments), and a punch of medial prefrontal cortex (mPFC) tissue including the anterior cingulate cortex (aCC) was taken using a 1-mm punch tool (Fine Science Tools, Foster City, CA). The tissues were lysed in RIPA buffer (10 mM Tris-HCl, pH 7.5, 150 mM NaCl, 2% Nonidet P-40, 5 mM EDTA, 0.1 mM phenylmethylsulfonyl fluoride, 1 mM β-glycerophosphate, 1 mM sodium orthovanadate, 10 mM sodium fluoride, 0.1 M SDS, 1% protease inhibitor cocktail-Sigma Aldrich), centrifuged at 12000*g* for 10 min, and the supernatant was collected. The protein was quantified with BRADFORD assay (BIORAD, Milan, Italy) and 30 μg of total protein was loaded on 12% acrylamide gel. After electroblotting onto a nitrocellulose membrane (Hybond-C Amersham Biosciences, Piscataway, NJ), the membranes were blocked in TBST (TBS + Tween 0.1%) containing 5% non-fat dried milk for 1 h at room temperature. Proteins including vGLUT1, vGLUT2, GluR1,

phosphorylated GluR1 (pGluR1) and PSD95 were visualized using appropriate primary antibodies (see the list below). All primary antibodies were diluted in milk 5% and incubated with the nitrocellulose blot overnight at 4 °C. Incubation with secondary peroxidase coupled anti-mouse, anti-rabbit or anti-guinea pig antibodies was performed by using the ECL system (Amersham, Arlington Heights, IL, U.S.A.). Anti-GAPDH antibody was used as a loading control for all experiments and all western blot data were normalized to GAPDH. Final figures were assembled by using Adobe Illustrator C6 (http://www.adobe.com/ca/products/illustrator.html) and quantitative analysis of acquired images was performed by using ImageJ (http://imagej.nih.gov/ij/).

Immunohistochemistry Mice were perfused transcardially with a 4% PFA solution for 1 h following the memory tests in context A. Their brains were removed and immersed overnight in the same solution. On the day after, they were transferred in a 30% sucrose solution prepared in PBS × 1 and cut with at cryostat in 40-μm slices. Three slices for each animal were used for immunofluorescence detection of vGLUT1 and PSD95 proteins. The primary antibodies were diluted in PBS × 1 with Triton 0.3% as follows: vGLUT1 1:400 and PSD95 1:100. Slices were incubated overnight at 4 °C with the primary antibody and, on the day after, were washed three times and then incubated with a mix solution of donkey anti-guinea pig Alexa 555 (1:500) and donkey anti-mouse Alexa 488 (1:500) secondary antibodies (Invitrogen) for 2 h at 4 °C. Slices were subsequently washed three times and, in the last wash, were incubated with a nuclear marker (Hoechst, 1:1000, Sigma-Aldrich) for 10 min followed by a further rinse. Sections were mounted on slides, air-dried and coverslipped using gel mount (Sigma Aldrich). Controls were performed by omitting the primary antibodies. Immunofluorescent sections were acquired with Zeiss confocal microscopy at magnification × 100.

Labelling and Co-Labelling of Synaptic Proteins vGLUT1 and PSD95 signals were detected separately from ten non-overlapping regions (10 × 10 μm squares) from each image. Regions were randomly selected avoiding Hoechst-labelled cell bodies. IMARIS (Imaris x64 Bitplane, v9.0.2) software was used for automatic detection and counting of vGLUT1 and PSD95 puncta and PSD95/vGLUT1 overlapping signals. For all the experiments, regions were analysed after establishing a detection threshold which was kept constant within each measurement.

Antibodies Antibodies used for of western blot and immunostaining were as follows: vGLUT1 (1:800; synaptic system; anti-guinea pig), vGLUT2 (1:100; synaptic system; anti-guinea pig), GluR1 (1:1000; Millipore; anti-rabbit), pGluR1Ser845 (1:1000; Millipore; anti-rabbit), PSD95 (1:100; Enzo Life Science; anti-mouse), GAPDH (1:5000; Calbiochem; anti-mouse).

mEPSCs Recordings Mice were deeply anaesthetised with isoflurane inhalation, decapitated and brains removed and immersed in cold 'cutting' solution (4 °C) containing (in mM): 126 choline, 11 glucose, 26 $NaHCO_3$, 2.5 KCl, 1.25 NaH_2PO_4, 10 $MgSO_4$, 0.5 $CaCl_2$ equilibrate with 95% O_2 and 5% CO_2. Coronal slices (300 μm) were cut with a vibratome (Leica) and then incubated in oxygenated artificial cerebrospinal fluid (ACSF) containing (in mM): 126 NaCl, 26 $NaHCO_3$, 2.5 KCl, 1.25 NaH_2PO_4, 2 $MgSO_4$, 2 $CaCl_2$ and 10 glucose; pH 7.4, initially at 32 °C for 1 h, and subsequently at room temperature, before being transferred to the recording chamber and maintained at 32 °C. Recordings were obtained from visually identified aCC pyramidal neurons in layer 2/3, easily distinguished by the presence of an emerging apical dendrite. Experiments were performed in the whole-cell configuration of the patch-clamp technique. Electrodes (tip resistance = 3–4 MΩ) were filled with an intracellular solution containing (in mM): K gluconate 135, KCl 4, NaCl 2, HEPES 10, EGTA 4, MgATP 4, NaGTP 2; pH adjusted to 7.3 with KOH; 290 mOsm. Whole-cell voltage-clamp recordings (− 70 mV holding potential) were obtained using a Muticlamp 700B (Axon CNS, Molecular Device). Spontaneous EPSCs recorded in the presence of TTX 1 μM (mEPSCs) were filtered at 1 kHz, digitized at 10 kHz and recorded on a computer using Digidata1440A and pClamp10 software (Molecular Device). Recordings were discarded if Rs changed 25% of its initial value. Experiments were carried out in the presence of GABA A receptor antagonist picrotoxin (100 μM). Miniature events were detected and analysed with Clampfit 10.4. The amplitude and frequency plots obtained for cells recorded in controls and after drug application were compared using the paired t test.

Spine Density Counting Thy1-GFP-M were perfused transcardially with a 4% PFA solution 24 h after the memory tests run in context A. The brains were removed and left overnight in the same solution. On the day after, they were transferred in a 30% sucrose solution prepared in PBS × 1 and cut with a cryostat in 40-μm slices. Spine density was analysed on aCC pyramidal neurons located in layers 2/3 delimited according to the Franklin and Paxinos [11] mouse atlas. Neurons (from 6 to 8 per animal) were selected, and high-resolution three-dimensional image stacks were collected by confocal laser-scanning microscopy (Zeiss LSM T-PMT, 1024 × 1024 pixels, Z-Stacks interval 0.2 μm; magnification × 100, 1.30 N.A., ZOOM 1). Acquired images were analysed by means of the Imaris Software (Bitplane, Oxford Instruments, UK). For each neuron, spine density was quantified along with five randomly selected segments of secondary and tertiary

branches of apical dendrites (segments > 20 μm in length). Segments were sampled 50 μm away from the soma in order to exclude the spine-depleted zone that arises from the cell body. Only protuberances with a clear connection to the dendrite shaft were counted as spines. The spine raw data were subsequently averaged for a neuron mean. All measurements were performed by an operator blind to the experimental conditions.

DREADDs-Mediated Cortical Activation Mice were anaesthetised with a mixture of titelamina/zolepam (Zoletil 100 mg/kg) and Xylazine (Rompun, 20 mg/kg) injected intraperitoneally at the dose of 50 mg/kg. They were mounted on a stereotaxic apparatus (David Kopf, USA) and, following a longitudinal-medial incision of the scalp, two holes were drilled in their skull in correspondence of the anterior cingulate cortex (antero-posterior + 0.8 mm from bregma; lateral ± 0.3 mm). A cannula (0.1 mm in diameter) connected to a micro-syringe (Hamilton) inserted in an infusion pump (Harvard apparatus, PHD, 2000) was descended dorsoventrally in each hemisphere (− 1.75 mm from the dura) to infuse bilaterally at a low rate (0.3 μL/min) 0.7 μL of a PBS × 2 solution containing a rAAV5/CaMKIIa-hM3D(Gq)-mCherry (University of North Carolina Vector Core) or the PBS × 2 solution alone (vehicle: VEH). The cannulae were left in place for an additional 6 min to allow the diffusion of the virus in the brain region. After a 3-week resting period, DREADDs mice were injected with Clozapine-N-oxide (CNO) or saline (SAL) while VEH mice were injected only with SAL. Injections were performed 30 min before training in context A, and 30 min before testing in context B to chemogenetically reactivate in the novel context the same population of transfected neurons activated during training. We then verified that DREADDs treatment could also anticipate post-synaptic remodelling of cortical synapses. Mice were sacrificed 1 h following exposure to context B and their brains were processed for dendritic spines counting in GFP-positive cortical neurons and for measurement of PSD95 levels. Additional control groups were run to verify that DREADDs/CNO or DREADDs and CNO alone do not promote post-synaptic remodelling in naïve mice and that the DREADDS/CNO treatment does not interfere with memory recall in the training context. DREADDs injection sites were controlled by mCherry immunochemistry visualization of the infected region (anti-mCherry antibody 1:200, abcam).

Statistical Analyses Differences in protein expression (western blot and immunostaining), miniature EPSCs (frequency and amplitude) and dendritic spines measured in trained and pseudo-trained mice after recent and remote recall were compared by means of two-tailed Student's tests. A two-way ANOVA with context (training vs novel) and recall time point (1 day vs 14 days) was carried out to evaluate the dependence of freezing scores from the context characteristics as a function of the duration of the training-to-test interval. One-way ANOVAs with treatment as the main factor were carried to assess the effect of DREADDs-mediated enhancement of cortical neuron activity on freezing scores at recent recall, and on dendritic spines in naïve conditions. Two-way ANOVAs with treatment (DREADDS/CNO vs DREADDS/SAL) and training condition (training vs pseudo-training) were carried out to compare spine density and PSD95 levels formation at recent recall. Fisher LSD post hoc tests were used for pair comparisons where necessary. Significance was set at $p < 0.05$.

Results

Mice Show Robust Freezing in the Training Context at Recent and Remote Recall

CFC-trained mice exhibited comparable freezing scores when they were returned to the training context 1 day or 14 days following training (C57, $t(9) = 0.86$, $p = 0.41$, Fig. 1a, b; Thy-1GFP, $t(8) = 0.34$, $p = 0.74$, Fig. 2a, b).

Remote, but Not Recent, Memory Associates with Coincident Enhancement of Pre- and Post-Synaptic Proteins in the aCC

The pre-synaptic proteins vGLUT1 and vGLUT2 and the post-synaptic proteins PSD95, GluR1 and pGluR1 present at excitatory synapses were measured by western blot in the medial prefrontal cortex following recent and remote memory recall. In the trained mice, vGLUT1 and vGLUT2 levels were increased following recent (vGLUT1, $t(6) = 2.45$, $p = 0.049$; vGLUT2, $t(6) = 2.46$, $p = 0.049$) and remote (vGLUT1, $t(7) = 3.20$, $p = 0.015$; vGLUT2, $t(7) = 2.40$, $p = 0.047$) recall. Differently, PSD95, GluR1 and pGluR1 levels were unchanged following recent recall training (PSD95, $t(15) =$

Fig. 1 Freezing scores and expression level of synaptic proteins in the anterior cingulate cortex at recent and remote recall in the training context. **a** Cartoon depicting the experimental protocol. **b** Histograms showing freezing scores (mean ± SEM) recorded in CFC-trained (blue bars) and pseudo-trained (grey bars) C57BL/6 mice during recent (empty bars) or remote (solid bars) recall. **c** Histograms showing the percentage increase (± SEM) of pre-synaptic (vGLUT1 and vGLUT2) and post-synaptic (PSD95, GluR1 and pGLUR1) protein expression in the trained mice relative to the pseudo-trained mice after recent (empty blue bars) or remote (solid blue bars) recall. **d** Representative immunoblots of pre- and post-synaptic proteins at each recall time point. **e–l** Immuno-detection of vGLUT1, PSD95 and of their co-localisation at recent (**e**, **f**, **g**) and remote (**h**, **i**, **j**) recall. Histograms depict the average number (mean ± SEM) of immune-reactive puncta detected in each experimental condition. **k–l** Representative images of vGLUT1 (red), PSD95 (green) and of their co-localisation in immunofluorescence-stained aCC sections following recent (**k**) and remote (**l**) memory recall (scale bars 6 μm). $*p < 0.05$, $**p < 0.01$, $***p < 0.005$

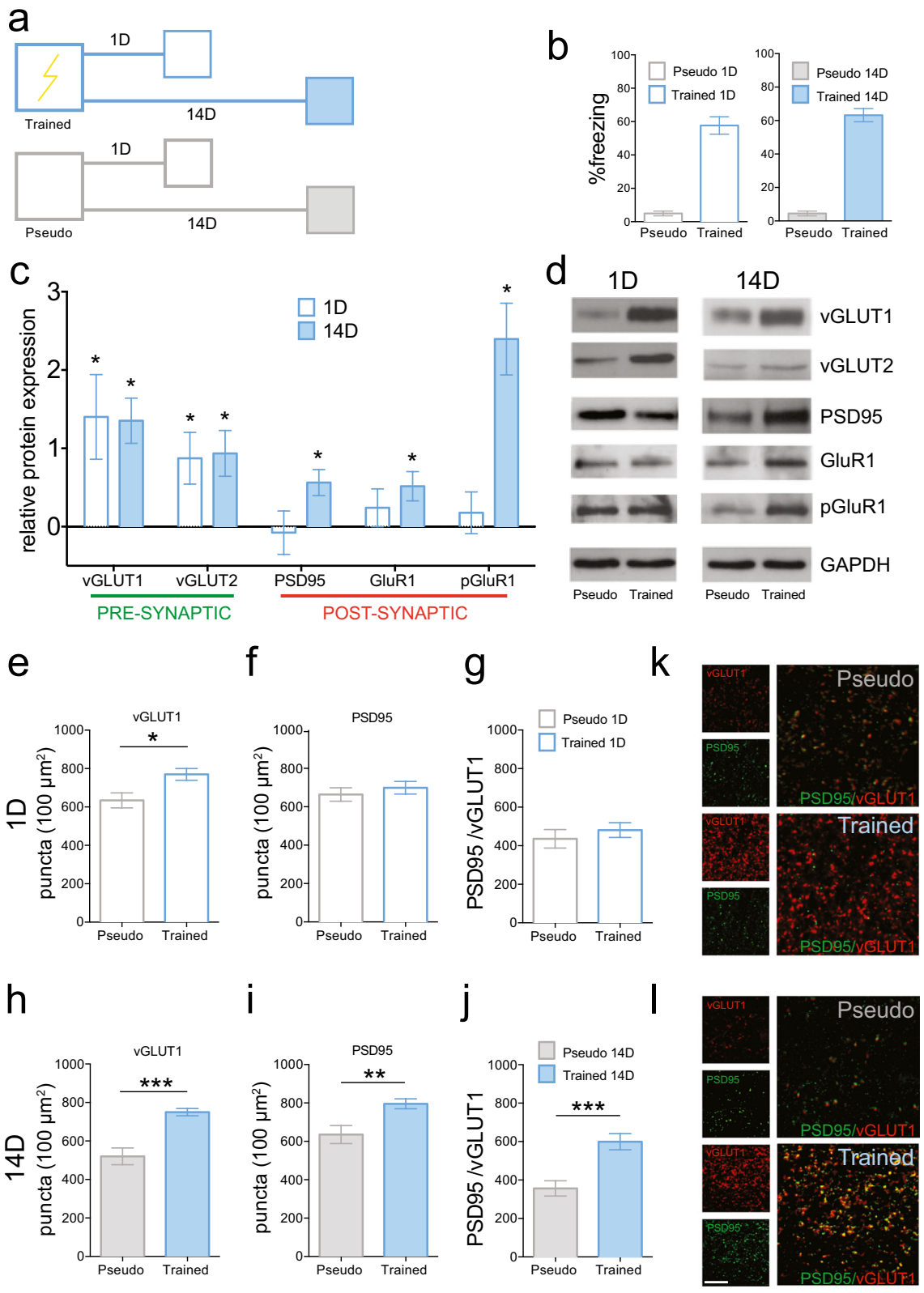
a
1D
Trained
14D
1D
Pseudo
14D
b
%freezing
Pseudo 1D
Trained 1D
Pseudo 14D
Trained 14D
Pseudo
Trained
c
relative protein expression
1D
14D
vGLUT1
vGLUT2
PSD95
GluR1
pGluR1
PRE-SYNAPTIC
POST-SYNAPTIC
d
1D
14D
vGLUT1
vGLUT2
PSD95
GluR1
pGluR1
GAPDH
Pseudo
Trained
e
vGLUT1
1D
puncta (100 µm²)
f
PSD95
g
PSD95 /vGLUT1
Pseudo 1D
Trained 1D
k
vGLUT1
PSD95
Pseudo
PSD95/vGLUT1
Trained
h
vGLUT1
14D
puncta (100 µm²)
i
PSD95
j
PSD95 /vGLUT1
Pseudo 14D
Trained 14D
l
vGLUT1
PSD95
Pseudo
PSD95/vGLUT1
Trained

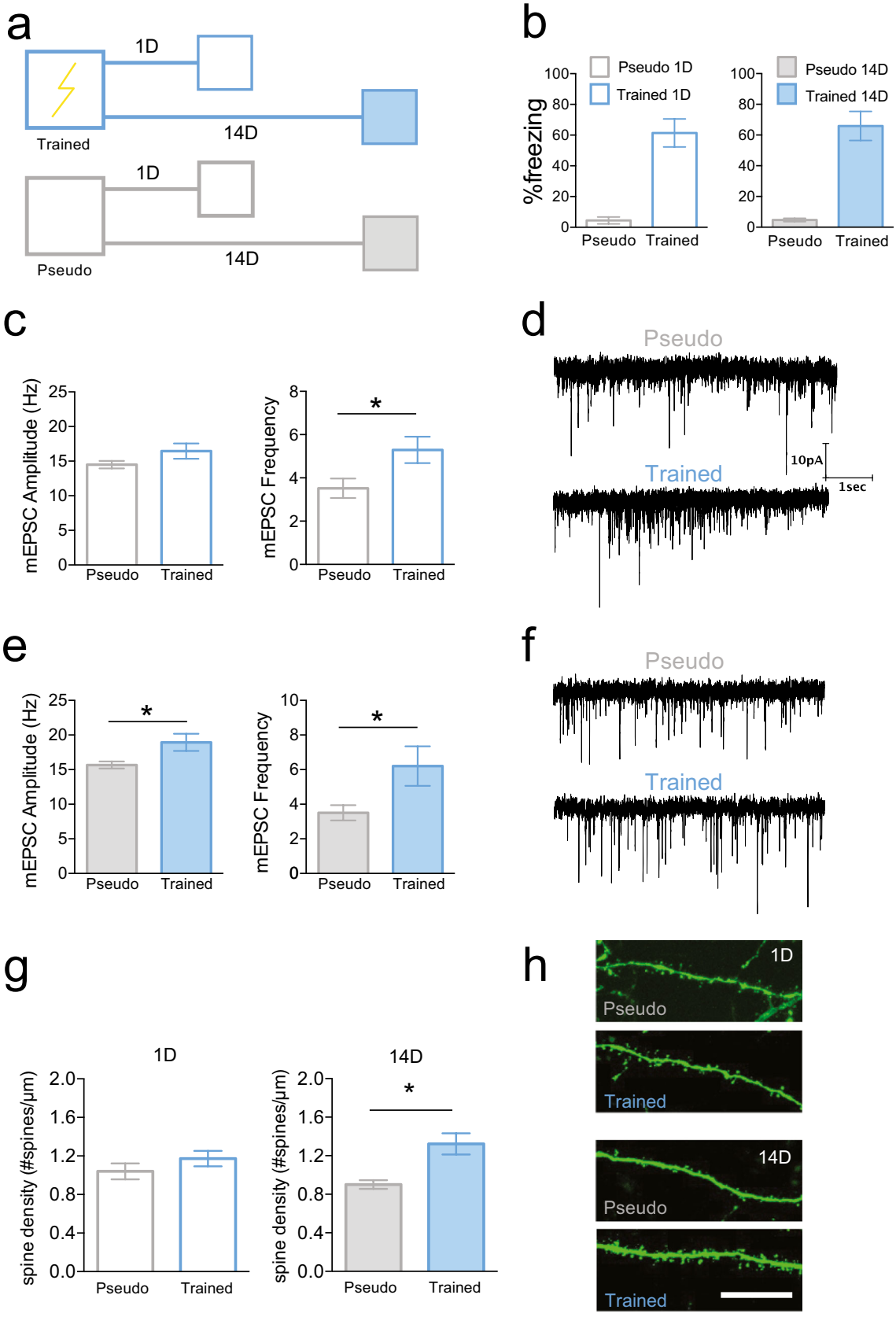
a
1D
Trained
14D
1D
Pseudo
14D
b
%freezing
Pseudo 1D
Trained 1D
Pseudo
Trained
Pseudo 14D
Trained 14D
Pseudo
Trained
c
mEPSC Amplitude (Hz)
Pseudo
Trained
mEPSC Frequency
*
Pseudo
Trained
d
Pseudo
Trained
10pA
1sec
e
mEPSC Amplitude (Hz)
*
Pseudo
Trained
mEPSC Frequency
*
Pseudo
Trained
f
Pseudo
Trained
g
1D
spine density (#spines/μm)
Pseudo
Trained
14D
*
spine density (#spines/μm)
Pseudo
Trained
h
1D
Pseudo
Trained
14D
Pseudo
Trained

◀ **Fig. 2** Freezing scores, miniature excitatory post-synaptic currents (mEPSCs) and dendritic spine density measured at recent and remote recall in the training context. **a** Cartoon depicting the experimental protocol. **b** Histograms show the mean freezing scores (± SEM) recorded in CFC-trained (blue bars) and pseudo-trained (grey bars) Thy-1GFP/C57 mice during recent (empty bars) and remote (solid bars) recall. **c** Histograms showing average values (± SEM) and **d** representative traces of amplitude and frequency of mEPSCs recorded in CFC-trained (empty blue bars) and pseudo-trained (empty grey bars) mice at recent recall. **e** Histograms showing average values (± SEM) and **f** representative traces of amplitude and frequency of mEPSCs recorded in CFC-trained (solid blue bars) and pseudo-trained (solid grey bars) at remote recall. **g** Histograms showing spine density (mean ± SEM) in layer 2/3 aCC neuron dendrites from CFC-trained (blue bars) and pseudo-trained (grey bars) mice following recent (empty bars) and remote (solid bars) recall. **h** Representative dendrite segments showing GFP-positive spines in each experimental condition. Scale bar 10 μm. *$p < 0.05$ (**j**)

0.16, $p = 0.87$; GluR1, $t(12) = 0.53$, $p = 0.61$; pGluR1, $t(8) = 0.78$, $p = 0.87$), but were increased following remote recall (PSD95, $t(8) = 2.491$, $p = 0.008$; GluR1, $t(10) = 2.54$, $p = 0.029$; pGluR1, $t(9) = 6.84$, $p = 0.0001$) (Fig. 1c, d). Immunostaining data confirmed western blot observations. A significant increase in the number of vGLUT1 ($t(17) = 2.55$, $p = 0.021$), but not of PSD95 ($t(17) = 0.70$, $p = 0.49$), puncta was detected following recent recall (Fig. 1e, f) whereas a concurrent increase of vGLUT1 ($t(26) = 5.06$, $p = 0.0001$) and PSD95 ($t(26) = 3.10$, $p = 0.005$) puncta was detected following remote recall (Fig. 1i, j). No increase in protein co-labelling was found in the trained mice following recent recall ($t(17) = 0.69$, $p = 0.49$, Fig. 1g, k) but co-labelling imputable to the concurrent increase in vGLUT1 and PSD95 was found following remote recall ($t(26) = 4.17$, $p = 0.003$, Fig. 1j, l).

Remote, but Not Recent, Memory Associates with Concurrent Enhancement of Frequency and Amplitude of Miniature EPSCs in aCC Neurons

Measurements of mEPSCs carried out after recent recall revealed that the frequency ($t(24) = 2.34$, $p = 0.028$) but not the amplitude ($t(24) = 0.13$, $p = 0.13$) was enhanced in aCC neurons from trained mice compared to pseudo-trained mice (Fig. 2c, d). Differently, both the mEPSCs frequency ($t(25) = 2.15$, $p = 0.042$) and amplitude ($t(25) = 2.38$, $p = 0.025$) were enhanced in aCC neurons after remote recall 14 (Fig. 2e, f).

Remote, but Not Recent, Memory Recall Associates with Dendritic Spine Growth in aCC Neurons

During memory consolidation, the modulation of synaptic strength is post-synaptically regulated by sequential formation of dendritic spines in the hippocampus and the anterior cingulate cortex [4, 5]. We confirmed our previous Golgi-staining data by showing that Thy1-GFP mice present an increase in spines of aCC neuron dendrites following remote, but not recent, recall (Fig. 2g, h). Specifically, the spine scores of trained and pseudo-trained mice were similar when the recall test was run 1 day post-training ($t(45) = 1.09$, $p = 0.28$) while more spines were counted in the trained mice when the recall test was run 14 days post-training ($t(39) = 2.83$, $p = 0.007$).

Remote, but Not Recent, Memory Is Independent from the Training Context

Context-specific memories which are formed shortly post-training become less specific with time [7]. Consistent with this view, statistical analysis revealed a context of recall × day interaction ($F(1,28) = 4.26$, $p = 0.049$). Post hoc pair comparisons then showed that mice exhibited more freezing in the training context than the novel context during recent recall, but the same amount of freezing during remote recall (Fig. 3). Confirming the contextual dependence of the recent memory representation, CFC-trained mice tested in context B on post-training day 1 were showed lower amount of freezing compared to the other groups ($p < 0.05$ for all post hoc comparisons).

DREADDs-Mediated Enhancement of aCC Neuron Activity Anticipates Expression of Schematic Memory

Intra-hippocampal injections of excitatory designer receptors exclusively activated by designer drug (DREADDs) with a neuron-specific promoter (CaMKIIα–HM3D) have been

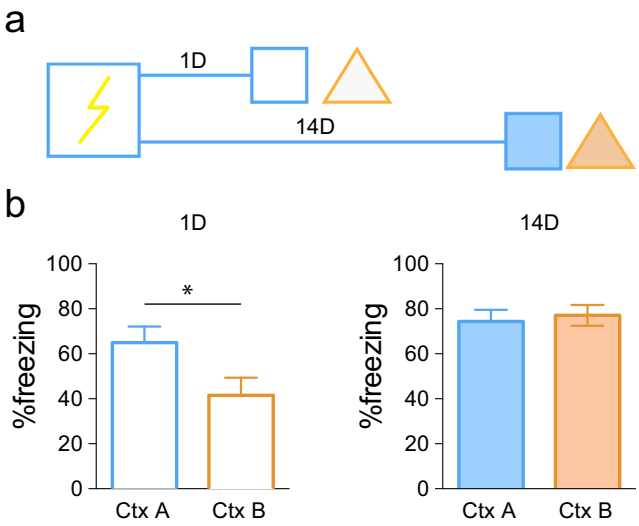

Fig. 3 Remote contextual fear memory generalizes to a novel context. **a** Cartoon depicting the experimental protocol. All mice were trained for contextual fear conditioning in a squared box (blue square). During recent (post-training day 1) or remote (post-training day 14) recall, mice were first returned to the training context (blue square) for a 4-min session and, 5 min later, were placed in a novel context (orange triangle) for the same duration. **b** Histograms show the time spent freezing (mean ± SEM) in the training (blue) or the novel (orange) context during recent (empty bars) and remote (solid bars) recall.*$p < 0.05$

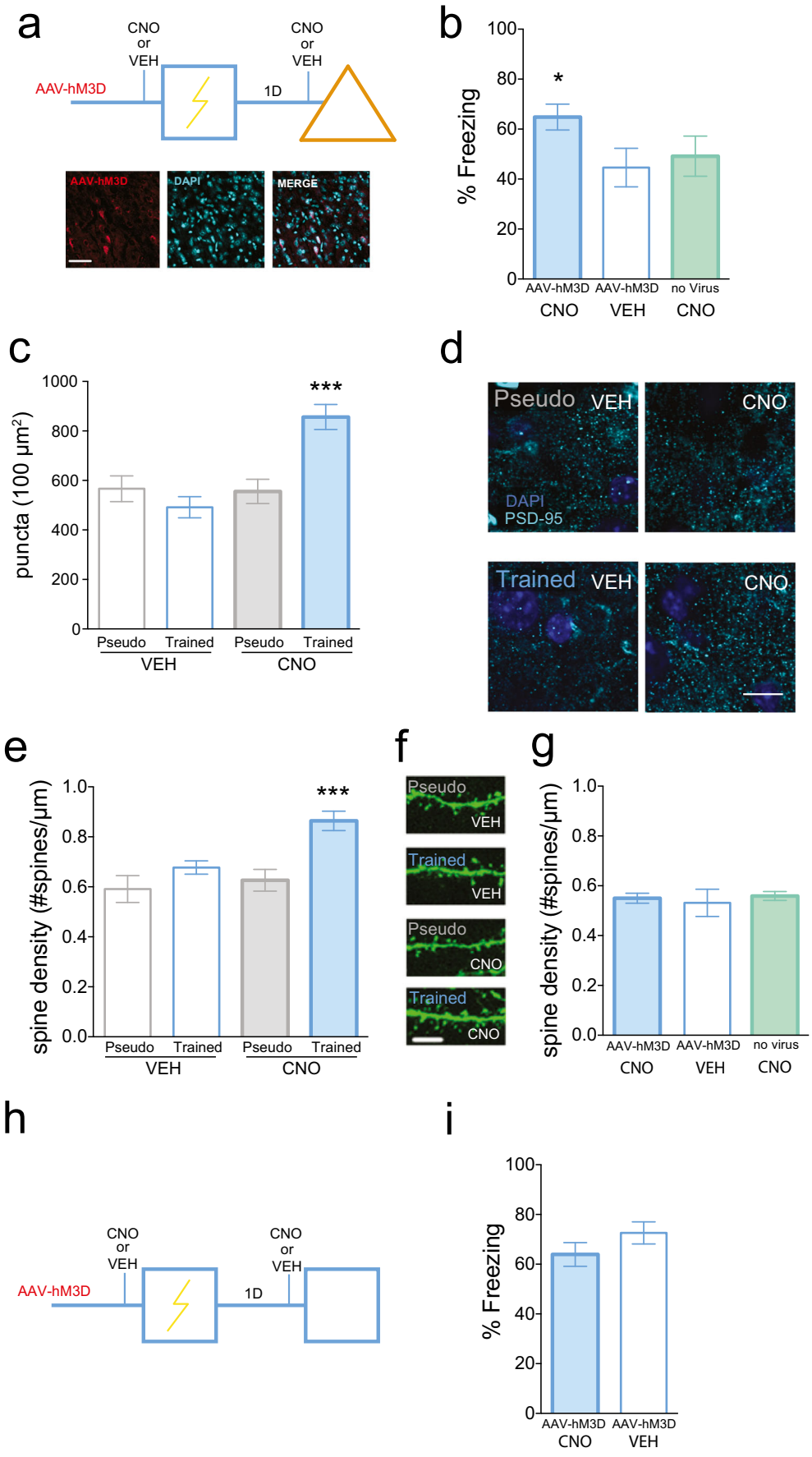
a
CNO or VEH
CNO or VEH
AAV-hM3D
1D
AAV-hM3D
DAPI
MERGE
b
% Freezing
100
80
60
40
20
0
*
AAV-hM3D CNO
AAV-hM3D VEH
no Virus CNO
c
puncta (100 µm²)
1000
800
600
400
200
0
***
Pseudo
Trained
Pseudo
Trained
VEH
CNO
d
Pseudo VEH
CNO
DAPI
PSD-95
Trained VEH
CNO
e
spine density (#spines/µm)
1.0
0.8
0.6
0.4
0.2
0.0
***
Pseudo
Trained
Pseudo
Trained
VEH
CNO
f
Pseudo VEH
Trained VEH
Pseudo CNO
Trained CNO
g
spine density (#spines/µm)
1.0
0.8
0.6
0.4
0.2
0.0
AAV-hM3D CNO
AAV-hM3D VEH
no virus CNO
h
CNO or VEH
CNO or VEH
AAV-hM3D
1D
i
% Freezing
100
80
60
40
20
0
AAV-hM3D CNO
AAV-hM3D VEH

◀ **Fig. 4** DREADDS-mediated increase of aCC neuron firing during training anticipates schematic memory expression and post-synaptic remodelling. **a** Cartoon depicting the experimental protocol with recent recall run in a novel context, and representative images of aCC neurons expressing hM3D-mCherry (red) counterstained with DAPI (blue) from Thy-1GFP-C57 mice (scale bar 50 μm). **b** Histograms showing the percentage of time (mean ± SEM) spent freezing in the novel context. DREADDS/CNO mice (blue bar) showed more freezing than DREADDs/vehicle (VEH) mice (white bar) and non-infected/CNO mice (green bar). **c** Histograms showing PSD95 expression levels (mean ± SEM) in the aCC following recent recall in the novel context. DREADDs/CNO-trained mice (solid blue bar) showed a higher number of PSD95 immuno-reactive puncta in the aCC than the three other groups (DREADDs/VEH-trained mice, solid grey bar; DREADDS/CNO pseudo-trained mice, empty blue bar; DREADDs/VEH pseudo-trained mice, empty grey bar). **d** Representative images of PSD95 immunostaining in each experimental condition (scale bar 10 μm). **e** Histograms showing dendritic spine density (mean ± SEM) on aCC neuron dendrites following recent recall in the novel context. DREADDs/CNO-trained mice (solid blue bar) exhibit more spines than the three other groups (DREADDs/VEH-trained mice, solid grey bar; DREADDs/CNO pseudo-trained mice, empty blue bar; DREADDs/VEH pseudo-trained mice, empty grey bar). **f** Representative dendrite segments showing GFP-positive spines in the four experimental conditions (scale bar 10 μm). **g** Histograms showing spine density (mean ± SEM) in aCC neuron dendrites from naïve DREADDs/CNO (solid blue bar), DREADDs/VEH (white bar) and non-infected/CNO (green bar) mice. Spine density does not vary between groups. **h** Cartoon depicting the experimental protocol with recent recall run in the training context. **i** Histograms showing the percentage of time (mean ± SEM) spent freezing in the training context by DREADDs/CNO (blue bar) and DREADDs/VEH (white bar) mice. The time spent freezing does not vary between groups. $*p < 0.05$, $***p < 0.005$

shown to increase hippocampal synaptic plasticity and transform a subthreshold learning event into long-term memory [12]. Considering that the DREADDs-mediated enhancement of synaptic efficacy modifies the quality of memory, we hypothesised that injecting excitatory DREADDs in the neocortex during CFC training and subsequent recent recall could anticipate generalization of memory to a novel context and bilateral remodelling of cortical synapses. To warrant that the same population of cortical neurons was activated during the formation of memory in one context and during its recent recall in another context, excitatory DREADDs were injected before both CFC training and recent testing. Specifically, DREADDs/CNO, DREADDs/VEH and VEH/CNO mice were trained in context A and directly placed in context B on the day after for recent recall (Fig. 4a). As shown in Fig. 4b, DREADDs/CNO mice exhibited more freezing in the novel context compared to the two other groups (significant effect of treatment ($F(2,22) = 3.59$, $p = 0.04$; DREADDs/CNO vs DREADDs/VEH or vs VEH/CNO, $p < 0.05$ for each pair comparison). Of note, no difference was detected in the low freezing scores of DREADDs/VEH and VEH/CNO thereby indicating that DREADDs or CNO alone has no effect on freezing. A control experiment (Fig. 4h, i) confirmed that DREADDs/CNO treatment does not affect the formation of memory when recent recall was run in the training context ($F(1,6) = 1.76$, $p = 0.23$; DREADDs/CNO vs DREADDs/VEH or vs VEH/CNO, $p > 0.05$).

DREADDs-Mediated Enhancement of aCC Neuron Firing Anticipates Post-Synaptic Remodelling

We then verified if DREADDs/CNO treatment promotes post-synaptic cortical remodelling after a recent recall in the novel context. In line with our hypothesis, post-synaptic plastic changes in aCC neurons were exclusively detected in the DREADDs/CNO-trained group. For PSD95 levels (Fig. 4h, i), a significant training × treatment interaction was found ($F(1,86) = 9.87$, $p = 0.023$), and pair comparisons showed that cortical PSD95 levels were higher in DREADDs/CNO-trained mice compared to DREADDs/VEH-trained mice ($p < 0.001$) and to DREADDs/CNO or DREADDs/VEH pseudo-trained mice ($p < 0.001$ for each comparison). For dendritic spines (Fig. 4e, f), a main effect of training ($F(1,51) = 15.3$, $p < 0.001$) indicates that, independently from the treatment condition, more aCC spines were counted in the trained than in the non-trained condition. However, subsequent pair-comparisons revealed that DREADDs/CNO-trained mice exhibited more dendritic spines than the three other groups ($p < 0.001$ for each paired comparison). A control experiment (Fig. 4g) confirmed that the DREADDs/CNO treatment did not increase cortical spines in naïve mice ($F(2,31) = 0.65$, $p = 0.52$).

Discussion

The time course of cortical recruitment in episodic memory formation is still a matter of debate [3, 4, 6, 13, 14]. On the one hand, the system consolidation theory holds that episodic memory traces initially formed in the hippocampus are progressively transferred to the neocortex with concurrent disengagement of the hippocampus. Within this framework, computational models assume that this transfer is slow because it depends on synergic interactions between a hippocampus-based system that rapidly encodes specific episodes and a neocortex-based system that gradually integrates multiple episodes and extracts their semantic structure [15]. Consistent with this view, memory-driven changes have been shown to accumulate progressively in the neocortex. For example, the number of c-fos-positive cortical neurons starts to augment significantly 5 days post-training and then shows a steady increase over successive weeks. Similarly, dendritic spines on aCC neuron dendrites are significantly enhanced 1 week following the conditioning and, although the net increase in spines rapidly stabilizes, single-neuron spine scores become gradually more homogeneous as memory matures over time [5]. Supporting the selective engagement of the hippocampus at the recent time point, chemogenetic blockade of

hippocampal activity by DREADDs prevents recent recall but spare remote recall [16]. Supporting its disengagement at the remote time point, early genes expression [17] and dendritic spines formation [4] which are increased upon recent recall return to baseline upon remote recall. Consistent with this view, plasticity mechanisms triggered by REM sleep have been shown to ensure the progressive corticalisation of hippocampus-dependent memories [18].

On the other hand, evidences showing that post-training disruption of cortical activity prevent recent recall [14] and optogenetic inhibition of CA1 neurons impairs remote recall [19] and suggest that the hippocampus and the neocortex could be concurrently involved at any stage of memory formation. Moreover, the report that CFC triggers a transcriptomic program accompanied by rapid structural and functional changes in local synaptic circuits of the mPFC indicates that the machinery supporting plastic changes is activated immediately after training [6]. Intriguingly, no detailed comparison of plastic changes occurring at cortical synapses during recent and remote recall is currently available. In particular, whether the properties of cortical remodelling vary over time and support distinct features of memory is unknown. To fill this gap, we investigated the molecular, physiological and structural alterations which develop in the medial prefrontal cortex following recent (1 day) and remote (14 days) memory recall with the objective of relating these alterations to time point specific properties of memory.

We first observed that recent recall was associated with pre-synaptic changes at cortical synapses. Specifically, the levels of the pre-synaptic markers of glutamatergic neurotransmission vGLUT1 and vGLUT2 were increased without a coincident increase in the post-synaptic markers GluR1, pGLUR1 and PSD95. Similarly, an augmentation in the number of vGLUT1, but not PSD95, immuno-reactive puncta was observed in the aCC, and no change in the density of GFP-positive spines was detected in aCC pyramidal neuron dendrites. Also, consistent with the Bero et al.'s data [6], the frequency, but not the amplitude, of mEPSCs was increased, which indicates an augmentation in the number of vesicles for release without the number of post-synaptic glutamatergic receptors is modified [20, 21]. Altogether, these observations reveal that excitatory neurotransmission is not significantly modified in the neocortex 24 h following CFC.

Conversely, bilateral remodelling of cortical synapses was found following a remote recall. The augmentation in vGLUT1 protein levels was accompanied by a coincident augmentation in GluR1, pGLUR1 and PSD95 levels determining a massive increase in the co-localisation of immunostained vGLUT1 and PSD95 puncta. Also, both the frequency and the amplitude of mEPSPs were increased and more dendritic spines were counted in aCC pyramidal neuron dendrites. The concurrent presence of an upregulation of the molecular machinery which mediates the strengthening of cortical synapses, and of an increase in dendritic spines which host excitatory synapses therefore reveals that the functionality and the density of cortical connections were selectively augmented in association with remote recall [22]. Of note, the existence of a direct, a plausibly causal, link between neo-formation of cortical spines and expression of remote CFC memory is supported by our previous data showing that preventing the formation of cortical spines by in situ aCC injections of the negative regulator of spinogenesis myocyte-enhanced factor 2 (MEF2) prevents remote recall [23].

Multiple evidences indicate that one main characteristic of episodic memories is that they do not retain their original content over time [7, 24–26]. In line with these reports, we found that mice tested for recent recall showed stronger freezing when returned to the training context than when exposed to a novel context. Differently, mice show comparable freezing in both contexts when tested for remote recall. Because the multiple memory trace theory predicts that novel traces, sharing progressively less common elements with the initial one, are continuously formed in the neocortex through slow variations in the density of cortico-cortical connections [27], the progressive augmentation in the number of c-fos-positive neurons and dendritic spines in the aCC [5] well aligns with the emergence of a schematic and flexible memory at the condition that newly formed spines host active, i.e. bilaterally remodelled, synapses. To confirm that post-synaptic remodelling of cortical neurons is a sufficient condition to disengage episodic memory from the training context, we enhanced activity of aCC neurons by chemogenetic DREADDs manipulations during both CFC-training in context A and recent recall in context B. Our hypothesis was that boosting activity of the same population of cortical neurons during memory encoding in one context, and recent recall in another context could favour the formation of a schematic memory and anticipate bilateral remodelling of cortical synapses. Consistently, we found that among mice expressing DREADDs in the aCC, those injected with the DREADDs activator CNO exhibited more freezing during recent recall in the novel context than those injected with SAL. Remarkably, no difference was found in the freezing scores of DREADDs/CNO and DREADDs/VEH-injected mice when the recent recall was run in the training context thereby confirming the hippocampus dependence of the context-specific recent memory representation. Then, in line with our hypothesis that by post-synaptic remodelling in the neocortex mediates expression of schematic memories, we found that aCC dendritic spines and PSD95 levels were increased in DREADDS/CNO-injected mice following recent recall in the novel context.

It is therefore apparent that plastic changes which develop in the neocortex immediately [6] or 1 day (present data) following CFC contribute to the tagging of cortical synapses but do not fully achieve the synaptic remodelling criteria that enable an episodic memory to acquire its remote schematic and

flexible properties. Consistent with this view, prefrontal cortex calcium-imaged engram cells detected 1 day following CFC were found not to be retrievable before several weeks thereby suggesting that a prefrontal memory engram is generated shortly post-training but in an immature form [28]. By showing that early pre-synaptic alterations need to be completed by post-synaptic alterations and de novo spine formation to disengage memory from its original context, our findings shed light on the synaptic properties required to support the formation of a mature prefrontal cortex engram whose function is to mediate rapid adaptation to partially similar experiences [29].

Author contributions These authors equally contributed to this work. GV, MAT and AP designed the experiments. GV and AB run behavioural, western blot/immunohistochemistry, and morphological experiments. SM and MG performed electrophysiological experiments. AP and GC carried out DREADDs experiments. MAT wrote the manuscript.

Funding Information This work was financially supported by a grant (AGESPAN) from CNR-National Research Council of Italy.

References

1. Cohen NJ, Poldrack RA, Eichenbaum H (1997) Memory for items and memory for relations in the procedural/declarative memory framework. Memory 5(1–2):131–178
2. Konkel A, Cohen NJ (2009) Relational memory and the hippocampus: representations and methods. Front Neurosci 3(2):166–174
3. Frankland PW, Bontempi B, Talton LE, Kaczmarek L, Silva AJ (2004) The involvement of the anterior cingulate cortex in remote contextual fear memory. Science 304(5672):881–883
4. Restivo L, Vetere G, Bontempi B, Ammassari-Teule M (2009) The formation of recent and remote memory is associated with time-dependent formation of dendritic spines in the hippocampus and anterior cingulate cortex. J Neurosci 29(25):8206–8214
5. Aceti M, Vetere G, Novembre G, Restivo L, Ammassari-Teule M (2015) Progression of activity and structural changes in the anterior cingulate cortex during remote memory formation. Neurobiol Learn Mem 123:67–71
6. Bero AW, Meng J, Cho S, Shen AH, Canter RG, Ericsson M, Tsai LH (2014) Early remodelling of the neocortex upon episodic memory encoding. Proc Natl Acad Sci U S A 111(32):11852–11857
7. Winocur G, Moscovitch M, Sekeres M (2007) Memory consolidation or transformation: context manipulation and hippocampal representations of memory. Nat Neurosci 10(5):555–557
8. Moscovitch M, Cabeza R, Winocur G, Nadel L (2016) Episodic memory and beyond: the hippocampus and neocortex in transformation. Annu Rev Psychol 67:105–134
9. Sekeres MJ, Winocur G, Moscovitch M (2018) The hippocampus and related neocortical structures in memory transformation. Neurosci Lett 680:39–53
10. Hardt O, Nadel L (2018) Systems consolidation revisited, but not revised the promise and limits of optogenetics in the study of memory. Neurosci Lett 680:54–59
11. Franklin and Paxinos (2001) The mouse brain in stereotaxic coordinates. Academic Press, San Diego
12. Lopez AJ, Kramar E, Matheos DP, White AO, Kwapis J, Vogel-Ciernia A, Sakata K, Espinoza M et al (2016) Promotor-specific effects of DREADD modulation on hippocampal synaptic plasticity and memory formation. J Neurosci 36(12):3588–3599
13. Lesburguères E, Gobbo OL, Alaux-Cantin S, Hambucken A, Trifilieff P, Bontempi B (2011) Early tagging of cortical networks is required for the formation of enduring associative memory. Science. 331(6019):924–928
14. Tse D, Takeuchi T, Kakeyama M, Kajii Y, Okuno H, Tohyama C, Bito H, Morris RG (2011) Schema-dependent gene activation and memory encoding in neocortex. Science. 333(6044):891–895
15. O'Reilly RC, Bhattacharyya R, Howard MD, Ketz N (2014) Cogn Sci 38(6):1229–1248
16. Varela C, Weiss S, Meyer R, Halassa M, Biedenkapp J, Wilson MA, Goosens KA, Bendor D (2016) Tracking the time-dependent role of the hippocampus in memory recal lusing DREADDs. PLoS One 11(5):e0154374
17. Frankland PW, Bontempi B (2005) The organization of recent and remote memory. Nat Rev Neurosci 6(2):119–130
18. Almeida-Filho DG, Queriroz CM, Riberiro S (2018) Memory corticalization triggered by REM-sleep: mechanisms of cellular and systems consolidation. Cell Mol Life Sci. https://doi.org/10.1007/s00018-018-2886-9
19. Goshen I, Brodsky M, Prakash R, Wallace J, Gradinaru V, Ramakrishnan C, Deisseroth K (2011) Dynamics of retrieval strategies for remote memories. Cell 147(3):678–689
20. Nonaka M, Doi T, Fujiyoshi Y, Takemoto-Kimura S, Bito H (2006) Essential contribution of the ligand-binding beta B/beta C loop of PDZ1 and PDZ2 in the regulation of postsynaptic clustering, scaffolding, and localization of postsynaptic density-95. J Neurosci 26(3):763–774
21. Sheng M, Kim MJ (2002) Postsynaptic signaling and plasticity mechanisms. Science. 298(5594):776–780
22. Yuste R (2011) Dendritic spines and distributed circuits. Neuron. 71(5):772–781
23. Vetere G, Restivo L, Cole CJ, Ross PJ, Ammassari-Teule M, Josselyn SA, Frankland PW (2011) Spine growth in the anterior cingulate cortex is necessary for the consolidation of contextual fear memory. Proc Natl Acad Sci U S A 108(20):8456–8460
24. Radulovic J, Kammermeier J, Spiess J (1998) Generalization of fear responses in C57BL/6N mice subjected to one-trial foreground contextual fear conditioning. Behav Brain Res 95(2):179–189
25. Wiltgen BJ, Silva AJ (2007) Memory for context becomes less specific with time. Learn Mem 14(4):313–317
26. Huckleberry KA, Ferguson LB, Drew MR (2016) Behavioral mechanisms of context fear generalization in mice. Learn Mem 23(12):703–709
27. Moscovitch M, Rosenbaum RS, Gilboa A, Addis DR, Westmacott R, Grady C, McAndrews MP, Levine B et al (2005) Functional neuroanatomy of remote episodic, semantic and spatial memory: a unified account based on multiple trace theory. J Anat 207(1):35–66
28. Kitamura T, Ogawa SK, Roy DS, Okuyama T, Morrissey MD, Smith LM, Redondo RL, Tonegawa S (2017) Engrams and circuits crucial for systems consolidation of a memory. Science 356(6333):73–78
29. Morrissey MD, Insel N, Takehara-Nishiuchi K (2017) Generalizable knowledge outweighs incidental details in prefrontal ensemble code over time. Elife 6